AIAA JOURNAL
Vol. 31, No. 2, February 1993

Thin-Walled Tubes Subjected to Combined Internal Pressure and Axial Load

Wei Jiang* and Kuang-Hsi Wu*
Florida International University, Miami, Florida 33199

Based on the kinematic hardening theory, this paper studies the elastic-plastic response of thin-walled tubes subjected to combined internal pressure and axial load. Exact closed-form solutions are obtained for linear loading paths. Stress-strain relationships, together with the corresponding movements of the yield center, are obtained for both monotonic and variable loadings. The response of the tube under nonproportional loading is shown to be path-dependent. However, due to the hardening, such path dependence will finally disappear and a hysteresis loop can always be reached under cyclic loading. The steady-state response can be elastic or can be a state of cyclic reversed plasticity depending on the amplitude of the cyclic load. Based on a thorough study of the elastic-plastic response of the thin-walled tube, this paper illustrates how the kinematic hardening rule describes the material behavior under nonproportional cyclic loadings.

I. Introduction

MANY mechanical and structural components are subjected to variable loads and temperatures. The stress analysis of such components often turns out to be very complicated whenever plastic deformation occurs. On the one hand, there can be a variety of different types of response, and the structure may fail because of high- or low-cycle fatigue or ratchetting. Classifying and determining the possible responses, keeping track of the variation of the stress-strain state as the load varies, and predicting the life of the structure is never easy. On the other hand, the elastic-plastic analysis relies heavily on the constitutive laws employed. The problem is that constitutive equations that accurately describe the realistic material behavior do not exist. Ideally, constitutive equations need to be developed, that would adequately represent actual material behavior and should, at the same time, be in a form convenient for mathematical manipulation or suitable for numerical computation. The classic hardening theory is based on the concept of loading surface which expands and moves as hardening develops. The isotropic hardening rule assumes that the loading surface expands without moving, whereas the kinematic hardening rule assumes that the loading surface translates as a rigid body. Since the isotropic hardening rule cannot reflect the Bauschinger effect and predicts no strain growth, which is a main concern in the cyclic loading environment, the kinematic hardening rule has been used extensively over the years. In fact, it appears that only the simplest linear kinematic hardening rule permits the analytical solutions in the complicated elastic-plastic and shakedown analysis of structures.

Experimental investigations (Refs. 1-5, for example), indicate that uniaxial experiments are not capable of revealing material behavior under nonproportional cyclic loading conditions. This has led to the concern of whether classic hardening models are able to predict the complex plastic deformation of materials. A thorough investigation is thus in demand to probe how the classic rules predict the material behavior under complex loading situations.

This paper, based on the simple kinematic hardening theory, presents a detailed study of the various transient and steady-state responses of thin-walled tubes subjected to combined internal pressure and axial load. Closed-form solutions are obtained for linear loading paths, and the stress-strain relationships under monotonic and variable loadings are found. In addition, the solution gives a picture of the plastic deformation and hardening, showing how the loading surface and its center move with the loads and when reversed plasticity will occur. The response of the tube is shown to be path-dependent, and some extra hardening is revealed. The solution then shows that, due to the kinematic hardening, such phenomena will finally disappear and a steady state, either one of the elastic shakedown or one of the cyclic reversed plasticity, can always be reached if the load cycles. Since the derivation is strictly based on the kinematic hardening rule, without any extra assumptions or simplifications, this investigation not only gives a thorough study of the elastic-plastic response of the thin-waled tube, but also illustrates how the kinematic hardening rule describes the material behavior under nonproportional cyclic loadings.

II. Kinematic Hardening Rule

According to the flow theory of plasticity, the total strain increment $d\epsilon_{ij}$ is made up of the elastic strain increment $d\epsilon^e_{ij}$ and the plastic strain increment $d\epsilon^p_{ij}$:

$$d\epsilon_{ij} = d\epsilon^e_{ij} + d\epsilon^p_{ij} \tag{1}$$

The elastic strain increment $d\epsilon^e_{ij}$ is related to the current stress increment $d\sigma_{ij}$ by the usual constitutive equations of isotropic elasticity:

$$d\epsilon^e_{ij} = (1/2G)[d\sigma_{ij} - (\nu/1 + \nu)\delta_{ij}\, d\sigma_{kk}] \tag{2}$$

where G is the shear modulus, ν the Poisson's ratio, and δ_{ij} the Kronecker symbol. The plastic deformation is assumed to obey the associated plastic flow law:

$$de^p_{ij} = d\lambda \frac{\partial F}{\partial \sigma_{ij}} \tag{3}$$

where de^p_{ij} is the plastic increment of the strain deviator

$$e_{ij} = \epsilon_{ij} - (1/3)\epsilon_{kk}\delta_{ij} \tag{4}$$

F is the yield function and $d\lambda$ an infinitesimal scalar factor. In the case of kinematic hardening, if the loading surface is given as

$$(S_{ij} - \alpha_{ij})(S_{ij} - \alpha_{ij}) = (2/3)\sigma_y^2 \tag{5}$$

Received Jan. 27, 1992; revision received June 25, 1992; accepted for publication July 27, 1992.

*Professor, Mechanical Engineering Department.

the plastic deviatoric strain increment

$$de_{ij}^p = d\lambda(S_{ij} - \alpha_{ij}) \tag{6}$$

In Eqs. (5) and (6), σ_y is the yield stress in tension,

$$S_{ij} = \sigma_{ij} - (1/3)\sigma_{kk}\delta_{ij} \tag{7}$$

is the stress deviator, and α_{ij} is the deviatoric back stress, which indicates the center of the loading surface. Some differential relations have been proposed for the determination of the increment $d\alpha_{ij}$ of the deviatoric back stress. In this paper we will use the simplest, but rather extensively used variant:

$$\alpha_{ij} = me_{ij}^p \tag{8}$$

where m is a kinematic hardening parameter characteristic of a given material.

Now differentiating Eq. (5) and making use of Eq. (8), one finds

$$(S_{ij} - \alpha_{ij})(dS_{ij} - m\, de_{ij}^p) = 0 \tag{9}$$

Then substituting de_{ij}^p into it according to Eq. (6), and using the yield condition, Eq. (5), one obtains

$$d\lambda = (1/2m\tau_y^2)(S_{ij} - \alpha_{ij})\, dS_{ij} \tag{10}$$

Finally, the plastic strain increment

$$de_{ij}^p = [(S_{kl} - \alpha_{kl})\, dS_{kl}/2m\tau_y^2](S_{ij} - \alpha_{ij}) \tag{11}$$

where in Eqs. (10) and (11)

$$\tau_y = \sigma_y/\sqrt{3} \tag{12}$$

is the yield stress in shear.

III. Thin-Walled Tubes Subjected to Internal Pressure and Axial Load

Consider a thin-walled tube of mean radius a and of thickness h that is subjected to an internal pressure p and an axial force P (Fig. 1). We assume that the geometry of the tube and the loading are such that the elastic or plastic buckling problem can be excluded in the discussion. Thus, in cylindrical coordinates (r, ϕ, z), all of the stresses except σ_ϕ and σ_z are negligible. For open-end tubes,

$$\sigma_\phi = pa/h \tag{13a}$$

$$\sigma_z = P/2\pi ah \tag{13b}$$

For closed-end tubes,

$$\sigma_\phi = pa/h \tag{14a}$$

$$\sigma_z = pa/2h + P/2\pi ah \tag{14b}$$

All of the normal strains ϵ_r, ϵ_ϕ, and ϵ_z have to be considered. The plastic volume change will be neglected.

Based on these nonzero stresses and strains, we can find the deviatoric stresses

$$S_{11} = -1/3(\sigma_\phi + \sigma_z) \tag{15a}$$

$$S_{22} = 1/3(2\sigma_\phi - \sigma_z) \tag{15b}$$

$$S_{33} = -1/3(\sigma_\phi - 2\sigma_z) \tag{15c}$$

the deviatoric back stresses

$$\alpha_{11} = -1/3(\alpha_\phi + \alpha_z) \tag{16a}$$

$$\alpha_{22} = 1/3(2\alpha_\phi - \alpha_z) \tag{16b}$$

$$\alpha_{33} = -1/3(\alpha_\phi - 2\alpha_z) \tag{16c}$$

and the deviatoric plastic strains

$$e_{11}^p = -(\epsilon_\phi^p + \epsilon_z^p) \tag{17a}$$

$$e_{22}^p = \epsilon_\phi^p \tag{17b}$$

$$e_{33}^p = \epsilon_z^p \tag{17c}$$

Then the yield condition, Eq. (5), becomes

$$(\sigma_\phi - \alpha_\phi)^2 - (\sigma_\phi - \alpha_\phi)(\sigma_z - \alpha_z) + (\sigma_z - \alpha_z)^2 = \sigma_y^2 \tag{18}$$

and the plastic flow law, Eq. (11), gives

$$d\epsilon_\phi^p = 1/6m\sigma_y{}^2[(2\sigma_\phi - \sigma_z) - (2\alpha_\phi - \alpha_z)]\{[(2\sigma_\phi - \sigma_z) - (2\alpha_\phi - \alpha_z)]\, d\sigma_\phi - [(\sigma_\phi - 2\sigma_z) - (\alpha_\phi - 2\alpha_z)]\, d\sigma_z\} \tag{19a}$$

$$d\epsilon_z^p = -(1/6m\sigma_y^2)[(\sigma_\phi - 2\sigma_z) - (\alpha_\phi - 2\alpha_z)]\{[(2\sigma_\phi - \sigma_z) - (2\alpha_\phi - \alpha_z)]\, d\sigma_\phi - [(\sigma_\phi - 2\sigma_z) - (\alpha_\phi - 2\alpha_z)]\, d\sigma_z\} \tag{19b}$$

Note that by the kinematic hardening rule, Eq. (8),

$$\alpha_\phi = m(2\epsilon_\phi^p + \epsilon_z^p) \tag{20a}$$

$$\alpha_z = m(\epsilon_\phi^p + 2\epsilon_z^p) \tag{20b}$$

Conversely,

$$\epsilon_\phi^p = (1/3m)(2\alpha_\phi - \alpha_z) \tag{21a}$$

$$\epsilon_z^p = -(1/3m)(\alpha_\phi - 2\alpha_z) \tag{21b}$$

Thus, by Eqs. (19) and (20),

$$d\alpha_\phi = (1/2\sigma_y^2)(\sigma_\phi - \alpha_\phi)\{[(2\sigma_\phi - \sigma_z) - (2\alpha_\phi - \alpha_z)]\, d\sigma_\phi - [(\sigma_\phi - 2\sigma_z) - (\alpha_\phi - 2\alpha_z)]\, d\sigma_z\} \tag{22a}$$

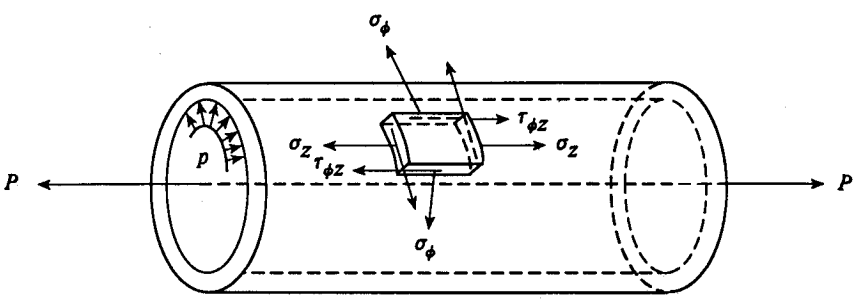

Fig. 1 Thin-walled tube under combined internal pressure and axial force.

$$d\alpha_z = (1/2\sigma_y^2)(\sigma_z - \alpha_z)\{[(2\sigma_\phi - \sigma_z) - (2\alpha_\phi - \alpha_z)]\, d\sigma_\phi - [(\sigma_\phi - 2\sigma_z) - (\alpha_\phi - 2\alpha_z)]\, d\sigma_z\} \quad (22b)$$

or

$$d(\sigma_\phi - \alpha_\phi) = -(1/2\sigma_y^2)[(\sigma_\phi - 2\sigma_z) - (\alpha_\phi - 2\alpha_z)] \times [(\sigma_z - \alpha_z)\, d\sigma_\phi - (\sigma_\phi - \alpha_\phi)\, d\sigma_z] \quad (23a)$$

$$d(\sigma_z - \alpha_z) = -(1/2\sigma_y^2)[(2\sigma_\phi - \sigma_z) - (2\alpha_\phi - \alpha_z)] \times [(\sigma_z - \alpha_z)\, d\sigma_\phi - (\sigma_\phi - \alpha_\phi)\, d\sigma_z] \quad (23b)$$

if use is made of the yield condition, Eq. (18).

To solve the tube problem, we introduce the following normalization:

$$\sigma = (\sigma_\phi + \sigma_z)/2\sigma_y \quad (24a)$$

$$\tau = (\sigma_\phi - \sigma_z)/2\tau_y \quad (24b)$$

$$\alpha = (\alpha_\phi + \alpha_z)/2\sigma_y \quad (25a)$$

$$\beta = (\alpha_\phi - \alpha_z)/2\tau_y \quad (25b)$$

$$\epsilon = E(\epsilon_\phi + \epsilon_z)/2(1 - \nu)\sigma_y \quad (26a)$$

$$\gamma = G(\epsilon_\phi - \epsilon_z)/\tau_y \quad (26b)$$

where σ and τ are normalized mean stress and maximum shear stress, α and β are normalized mean back stress and maximum back shear stress, and ϵ and γ are corresponding strains. By means of these normalized stresses, the yield condition, Eq. (18), and the differential equations, Eqs. (23), can be greatly simplified:

$$(\sigma - \alpha)^2 + (\tau - \beta)^2 = 1 \quad (27)$$

$$d(\sigma - \alpha) = (\tau - \beta)[(\tau - \beta)\, d\sigma - (\sigma - \alpha)\, d\tau] \quad (28a)$$

$$d(\tau - \beta) = -(\sigma - \alpha)[(\tau - \beta)\, d\sigma - (\sigma - \alpha)\, d\tau] \quad (28b)$$

Note that a differentiation of the yield condition, Eq. (27), gives

$$(\sigma - \alpha)\, d(\sigma - \alpha) + (\tau - \beta)\, d(\tau - \beta) = 0 \quad (29)$$

and therefore, the two equations in Eq. (28) are in fact identical.

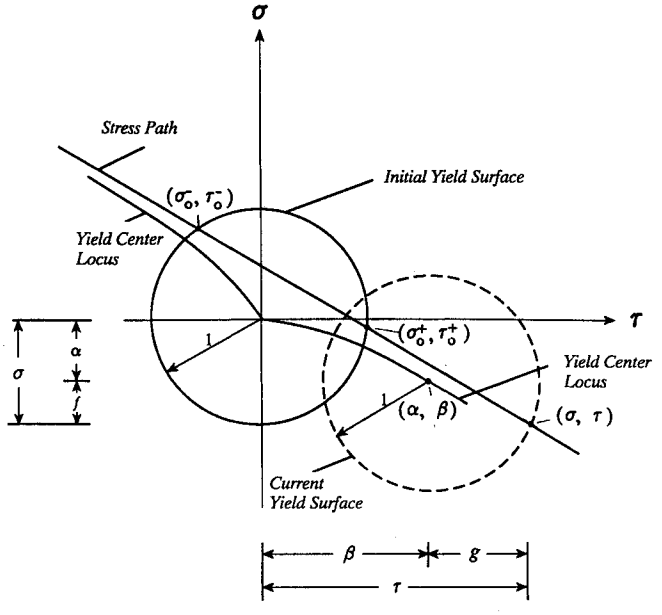

Fig. 2 Linear stress path ($\sigma = A - B\tau$, $B > 0$).

After Eqs. (28) are solved, the stresses and strains can be found as follows:

$$\sigma_\phi = \sigma_y\sigma + \tau_y\tau \quad (30a)$$

$$\sigma_z = \sigma_y\sigma - \tau_y\tau \quad (30b)$$

$$\epsilon_\phi = [\sigma_y(1 - \nu)\epsilon + \tau_y(1 + \nu)\gamma]/E \quad (31a)$$

$$\epsilon_z = [\sigma_y(1 - \nu)\epsilon - \tau_y(1 + \nu)\gamma]/E \quad (31b)$$

IV. Linear Stress Path—Monotonic Loading

To solve Eqs. (28), some loading path should be given. In this paper, we will consider the linear loading path:

$$p = C + DP \quad (32)$$

or, equivalently, the stress path

$$\sigma = A - B\tau \quad (33)$$

where in Eqs. (32) and (33) C and D are two constants, and

$$A = aC/(1 - 2\pi a^2 D)h\sigma_y \quad (34a)$$

$$B = 1 + 2\pi a^2 D/\sqrt{3}(1 - 2\pi a^2 D) \quad (34b)$$

for open-end tubes and

$$A = aC/(1 - \pi a^2 D)h\sigma_y \quad (35a)$$

$$B = (1 + 3\pi a^2 D)/\sqrt{3}(1 - \pi a^2 D) \quad (35b)$$

for closed-end tubes. In experimental investigations, we often use tubes subjected to sustained internal pressure and cyclic axial load. Then Eqs. (34) and (35) both reduce to

$$A = ap/h\sigma_y \quad (36a)$$

$$B = 1/\sqrt{3} \quad (36b)$$

In general, we assumed that $0 < A < 1$, whereas B can be any real number.

In the $\sigma - \tau$ plane (Fig. 2), the stress path intersects the initial yield surface at

$$\sigma_0^+ = (A - B\sqrt{1 + B^2 - A^2})/(1 + B^2) \quad (37a)$$

$$\tau_0^+ = (AB + \sqrt{1 + B^2 - A^2})/(1 + B^2) \quad (37b)$$

and

$$\sigma_0^- = (A + B\sqrt{1 + B^2 - A^2})/(1 + B^2) \quad (38a)$$

$$\tau_0^- = (AB - \sqrt{1 + B^2 - A^2})/(1 + B^2) \quad (38b)$$

where plastic deformation will first start.

Along the stress path, Eq. (33), Eqs. (28) become

$$d(\tau - \beta) = (\sigma - \alpha)[(\sigma - \alpha) + B(\tau - \beta)]\, d\tau \quad (39)$$

The coordinates of the yield center can be found from this differential equation as

$$\alpha = \sigma - f \quad (40a)$$

$$\beta = \tau - g \quad (40b)$$

where

$$f = -(BX^2 - 2X - B)/\sqrt{1 + B^2}(X^2 + 1) \quad (41a)$$

$$g = (X^2 + 2BX - 1)/\sqrt{1 + B^2}(X^2 + 1) \quad (41b)$$

in which

$$X = X_0 \exp[\sqrt{1 + B^2}(\tau - \tau_0)] \tag{42}$$

Depending on the loading direction, the initial value X_0 can be X_0^+ or X_0^- as follows:

$$X_0^+ = (\sqrt{1 + B^2} + \sqrt{1 + B^2 - A^2})/A \tag{43a}$$

$$X_0^- = (\sqrt{1 + B^2} - \sqrt{1 + B^2 - A^2})/A \tag{43b}$$

By Eqs. (21), the plastic strains

$$\epsilon^p = [E/3m(1 - \nu)]\alpha \tag{44a}$$

$$\gamma^p = (2G/m)\beta \tag{44b}$$

By Eq. (2), the elastic strains

$$\epsilon^e = \sigma \tag{45a}$$

$$\gamma^e = \tau \tag{45b}$$

A superposition thus yields the stress-strain relationships for the tube subjected to combined internal pressure and axial loads:

$$\epsilon = \{1 + [E/3m(1 - \nu)]\}\sigma - [E/3m(1 - \nu)]f \tag{46a}$$

$$\gamma = [1 + (2G/m)]\tau - (2G/m)g \tag{46b}$$

To investigate how these two equations describe material behavior, we first derive the following derivatives:

$$\frac{d\alpha}{d\tau} = -\frac{B(X^2 - X_4)(X - X_2)(X + X_2^{-1})}{(X^2 + 1)^2} \tag{47a}$$

$$\frac{d^2\alpha}{d\tau^2} = -\frac{2\sqrt{1 + B^2}X(X - X_3)(X + X_3^{-1})(X - X_7)(X + X_7^{-1})}{(X^2 + 1)^3} \tag{47b}$$

$$\frac{d\beta}{d\tau} = \frac{(X^2 - X_4)(X - X_6)(X + X_6^{-1})}{(X^2 + 1)^2} \tag{48a}$$

$$\frac{d^2\beta}{d\tau^2} = -\frac{2B\sqrt{1 + B^2}X(X - X_1)(X + X_1^{-1})(X - X_5)(X + X_5^{-1})}{(X^2 + 1)^3} \tag{48b}$$

where

$$X_1 = [\sqrt{2(b^2 + 1)} + (b + 1)]/(b - 1) \tag{49a}$$

$$X_2 = (b + 1)/(b - 1) \tag{49b}$$

$$X_3 = (\sqrt{b^2 + 1} + 1)/b \tag{49c}$$

$$X_4 = 1 \tag{49d}$$

$$X_5 = [\sqrt{2(b^2 + 1)} - (b - 1)]/(b + 1) \tag{49e}$$

$$X_6 = 1/b \tag{49f}$$

$$X_7 = \sqrt{b^2 + 1} - b \tag{49g}$$

in which

$$b = \sqrt{1 + B^2} + B \tag{50}$$

The stress τ_i corresponding to X_i can be found from Eq. (42):

$$\tau = \tau_0 + [1/(\sqrt{1 + B^2})] \ln(X/X_0) \tag{51}$$

Consider first the case when $B > 0$. For this kind of stress path (Fig. 2)

$$X_7 < X_6 < X_5 < X_4 < X_3 < X_2 < X_1 \tag{52}$$

Figures 3a and 3b give the variations of the functions (f, g) and Figs. 3c and 3d show the variations of the coordinates (α, β) of the yield center. The coordinate α monotonically decreases in the regions $\tau < \tau_4$ and $\tau > \tau_2$ and monotonically increases in the region $\tau_4 < \tau < \tau_2$. It is concave downward in regions $\tau < \tau_7$ and $\tau > \tau_3$, and concave upward in region $\tau_7 < \tau < \tau_3$. It approaches asymptotically straight lines with a slope of $-B$ for large stress. The coordinate β monotonically increases in regions $\tau < \tau_6$ and $\tau > \tau_4$, and monotonically decreases in region $\tau_6 < \tau < \tau_4$. It is concave downward in $\tau < \tau_5$ and $\tau > \tau_1$ and concave upward in $\tau_5 < \tau < \tau_1$. It approaches asymptotically straight lines in a 45-deg direction when stress tends to infinity.

Now we can investigate the maximum shear stress-strain relationship. The mean stress-strain relationship will not be discussed because of the similarity.

Suppose first that the tube is loaded in the positive direction. Plasticity will start when the stress τ reaches τ_0^+, or equivalently, when the X function reaches its initial value X_0^+. Then the stresses and the strains will follow the relationship, Eqs. (46). By Eqs. (43) and (49), we can find that

$$X_0^+ > X_4 \tag{53}$$

Since the X function monotonically increases with the stress, it will always be greater than X_4 due to Eq. (53), so that from the characteristics of the β function,

$$\frac{d\gamma}{d\tau} = 1 + \frac{2G}{m}\frac{d\beta}{d\tau} > 0 \tag{54}$$

Equation (54) shows that the shear stress-strain curve is always monotonically increased, as it should be.

On the other hand, we can find that

$$X_0^+ \gtrless X_1, \quad \text{if} \quad A \lesseqgtr \sqrt{\frac{\sqrt{1 + B^2}(\sqrt{1 + B^2} - 1)}{2}} \tag{55}$$

As a result, if $X_0^+ > X_1$

$$\frac{d^2\gamma}{d\tau^2} < 0 \tag{56}$$

and if $X_0^+ < X_1$

$$\frac{d^2\gamma}{d\tau^2} \gtrless 0, \quad \text{if} \quad X \lesseqgtr X_1 \quad \text{or} \quad \tau \lesseqgtr \tau_1 \tag{57}$$

In other words, if $X_0^+ > X_1$, the shear stress-strain curve is solely concave upward (Fig. 4a); if $X_0^+ < X_1$, the stress-strain curve will be concave downward first, before it changes to become concave upward (Fig. 4b). Since the shear stress-strain curve is always monotonically increased, it exhibits a yield plateau near the stress τ_1. This type of curve appears to resemble the experiment curve better.

When stress increases, the stress-strain curve asymptotically approaches the asymptote

$$\gamma = [1 + (2G/m)]\tau - (2G/m)g_\infty \tag{58}$$

where

$$g_\infty = 1/\sqrt{1 + B^2} \tag{59}$$

This asymptote intersects the elastic stress-strain curve,

$$\tau = \gamma \tag{60}$$

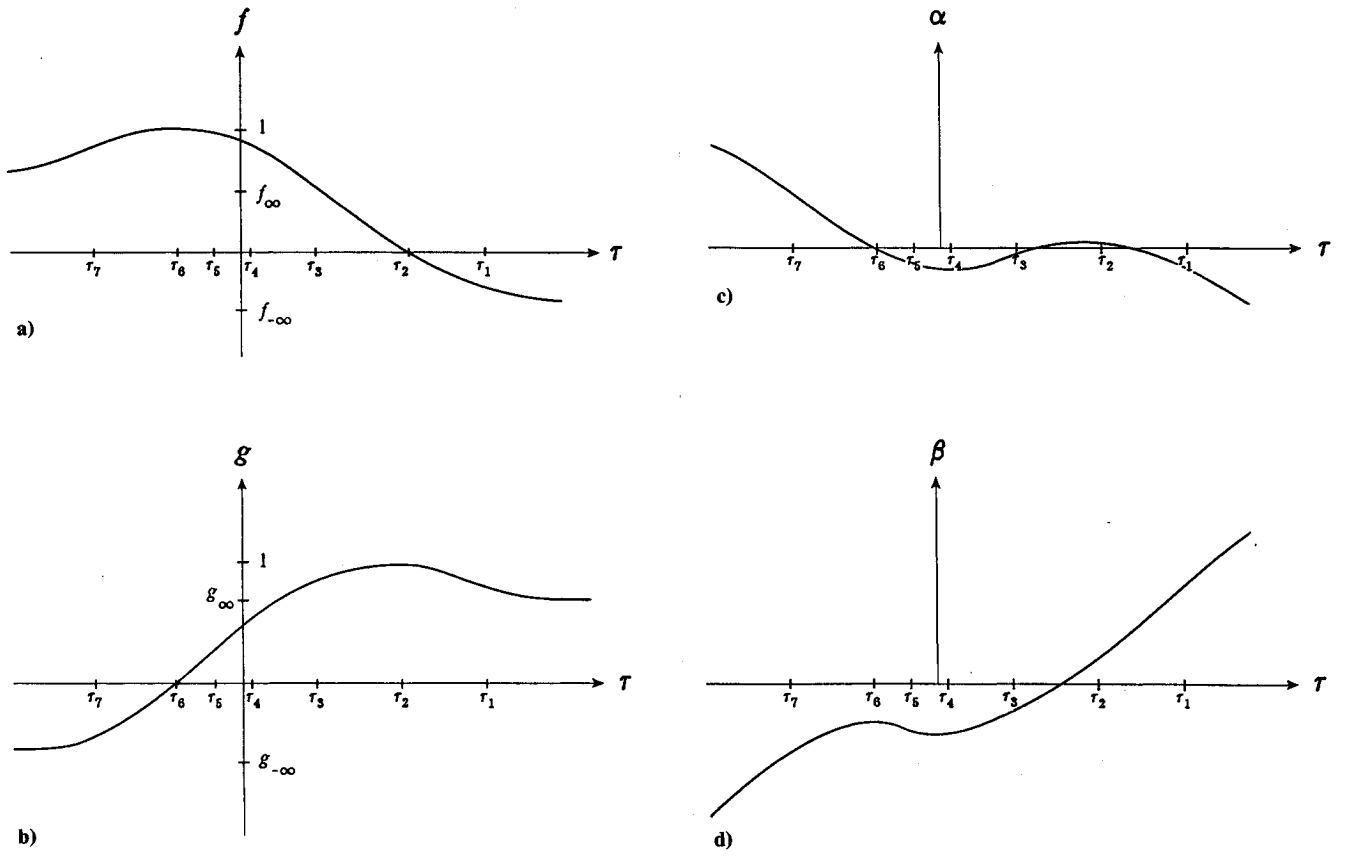

Fig. 3 Functions f, g, α, and β, linear stress path ($\sigma = A - B\tau$, $B > 0$).

at point (g_∞, g_∞). By Eqs. (37) and (59),

$$\tau_0^+ - g_\infty = -\frac{A^2[A^2(1+B^2) - 4B^2]}{\sqrt{1+B^2}(AB + \sqrt{1+B^2} - \sqrt{1+B^2-A^2})[(2-A^2)\sqrt{1+B^2} + 2\sqrt{1+B^2-A^2}]} \tag{61}$$

Note that the shear stress-strain curve is concave upward for large shear stress. Consequently, it can approach the asymptote only from above. If $A < 2B/\sqrt{1+B^2}$, Eq. (61) shows that $\tau_0^+ > g_\infty$. The plastic stress-strain curve falls entirely above the asymptote. It can be a solely concave upward curve (Fig. 4a), or can be a concave downward-upward curve (Fig. 4b), depending upon whether A is less or greater than the value

$$\sqrt{\sqrt{1+B^2}(\sqrt{1+B^2}-1)/2}$$

On the other hand, if $A > 2B/\sqrt{1+B^2}$, Eq. (61) gives $\tau_0^+ < g_\infty$. The initial part of the plastic stress-strain curve stays below the asymptote, so that the shear stress-strain curve cannot approach the asymptote if it is solely concave upward. This kind of nonapproachable possibility, however, does not exist. In fact, since $A < 1$, B should be less than $1/\sqrt{3}$ to make $A > 2B/\sqrt{1+B^2}$. In such a case, we can prove that

$$\sqrt{\frac{\sqrt{1+B^2}(\sqrt{1+B^2}-1)}{2}} < \frac{2B}{\sqrt{1+B^2}} \tag{62}$$

and consequently

$$A > \sqrt{\frac{\sqrt{1+B^2}(\sqrt{1+B^2}-1)}{2}}, \quad \text{or} \quad X_0^+ < X_1 \tag{63}$$

In other words, in the case of $\tau_0^+ < g_\infty$, the shear stress-strain curve will always be concave downward first, and then change to be concave upward, approaching the asymptote from above (Fig. 4c).

Suppose next that the tube is loaded in the negative direction. Plasticity will start when the stress τ reaches τ_0^-, or equivalently, when the X function reaches its initial value X_0^-. In such a case, we can find from Eqs. (43) and (49) that

$$X_0^- < X_6 \tag{64}$$

so that from the characteristics of the β function,

$$\frac{d\gamma}{d\tau} > 0 \tag{65a}$$

$$\frac{d^2\gamma}{d\tau^2} < 0 \tag{65b}$$

If the stress keeps growing, the shear stress-strain curve approaches the asymptote

$$\gamma = [1 + (2G/m)]\tau - (2G/m)g_{-\infty} \tag{66}$$

where

$$g_{-\infty} = -1/\sqrt{1+B^2} = -g_\infty \tag{67}$$

Note that this asymptote intersects the elastic stress-strain curve, Eq. (60), at point $(g_{-\infty}, g_{-\infty})$. Note also that by Eqs. (38) and (67)

$$\tau_0^- - g_{-\infty} = [AB + (\sqrt{1+B^2} - \sqrt{1+B^2-A^2})]/(1+B^2) > 0 \tag{68}$$

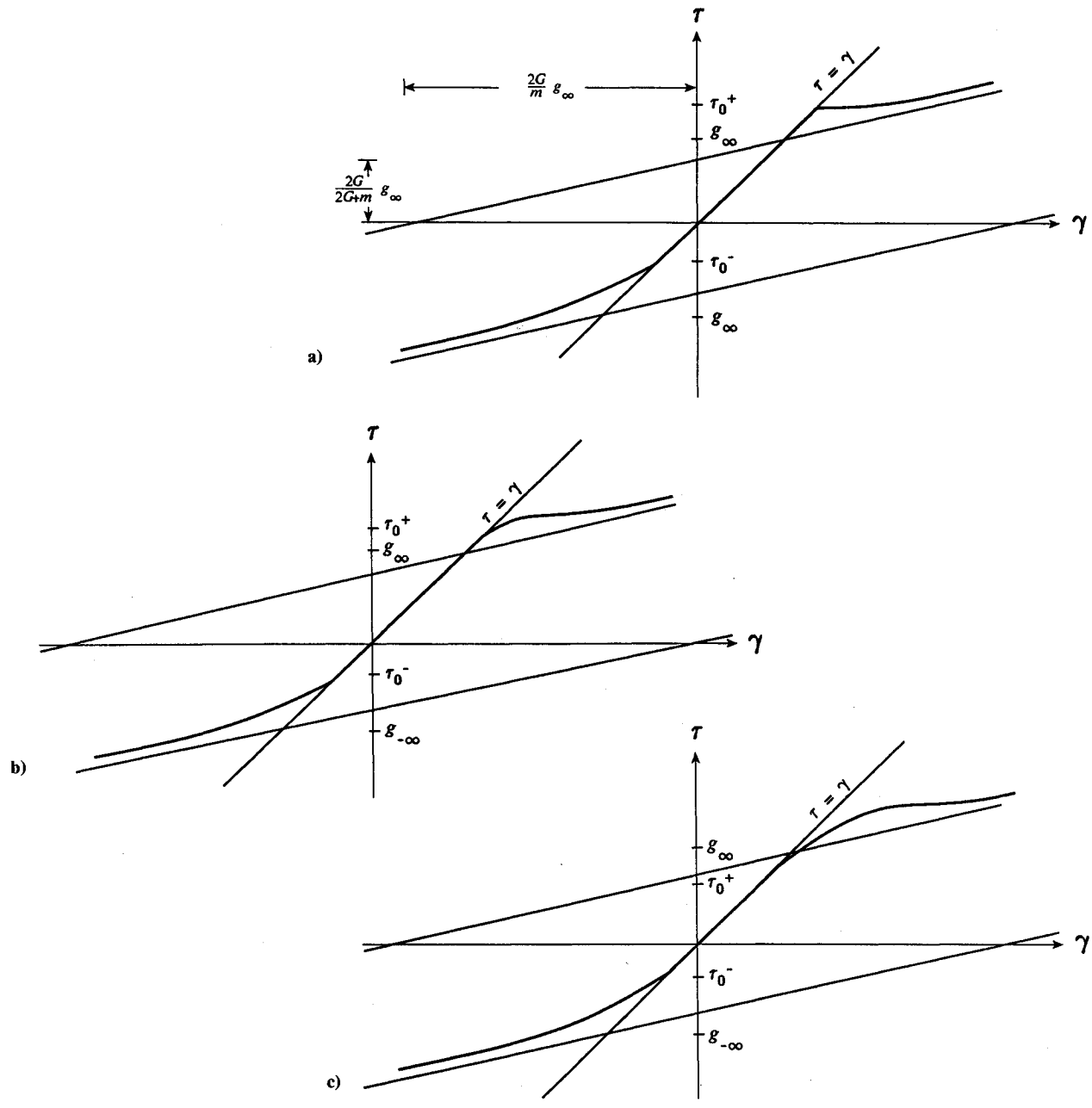

Fig. 4 Shear stress-strain relationship, linear stress path ($\sigma = A - B\tau$, $B > 0$).

Thus, we can see that in the negative loading direction, Eq. (46) gives a shear stress-strain curve that is monotonically increased and concave upward, bounded by the elastic stress-strain relationship, Eq. (60), and the asymptote, Eq. (66), from right and from below (Fig. 4). This kind of stress-strain relationship is thus quite conventional.

When plastic deformation occurs, the yield center begins to move. Equation (40) indicates that the movement of the yield center lags behind that of the loading point by f in the vertical direction and by g in the horizontal direction (Fig. 2). For large stress τ, f approaches $\mp B/\sqrt{1+B^2}$, while g approaches $\pm 1/\sqrt{1+B^2}$. As a result, the yield center locus will asymptotically approach the stress path when the shear stress increases to infinity.

It is seen from this discussion that along the stress path, Eq. (33), the tube responds differently in the positive loading direction and in the negative loading direction. Such differences disappear only when $B = 0$, that is, only when the stress path is parallel to the τ axis (Fig. 5). At that time, $X_1 = \infty$,

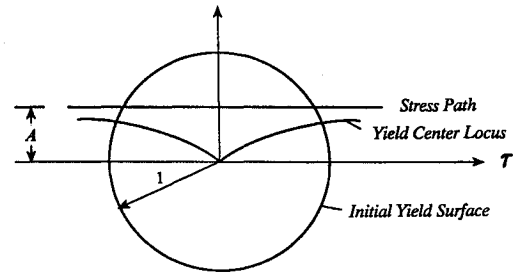

Fig. 5 Linear stress path ($\sigma = A$).

$\tau_1 = \infty$, and $\tau_0^+ < g_\infty$, so that the positive loading shear stress-strain curve becomes solely concave downward and remains entirely below the asymptote, Eq. (58). It is easy to show that for such a stress path, the shear stress-strain curves for positive and negative loading directions are antisymmetric with

respect to the origin 0 (Fig. 6), and the tube will have the same response, apart from a sign, to either loading direction.

Note that the characteristics of the shear stress-strain curve for a stress path with $B<0$ in the positive (negative) loading direction is similar to those for a stress path with $B>0$ in the negative (positive) loading direction. In fact we can prove that the tube exhibits the same behavior along stress paths that are symmetric to the σ axis.

V. Linear Stress Path—Variable Loading

Suppose that after the tube is loaded in the tensile direction to the loading point 2, unloading starts (Fig. 7). During the unloading, the yield surface will not move until the loading point hits the yield surface at point 3, when reversed plasticity takes place. In the τ-γ plane (Fig. 8), the unloading part follows the straight line 2-3, representing an elastic response. After the loading point 3, negative plastic deformation occurs, and the response of the tube begins to be controlled by the differential equations, Eq. (39), again. The new yield center and the new stress-strain relationship can still be represented by Eqs. (40–46), but with new initial conditions.

Let (σ_i, τ_i), (α_i, β_i), X_i, and (f_i, g_i) be the values of the corresponding functions at the loading point i, where the loading direction changes. It can be seen from Fig. 7 that reversed plasticity will occur when the stress increment at the loading point 2 satisfies the yield condition:

$$(\sigma_2 + \Delta\sigma_2 - \alpha_2)^2 + (\tau_2 + \Delta\tau_2 - \beta_2)^2 = 1 \tag{69}$$

or

$$(\Delta\sigma_2 + f_2)^2 + (\Delta\tau_2 + g_2)^2 = 1 \tag{70}$$

Note that

$$f^2 + g^2 = 1 \tag{71}$$

and

$$\Delta\sigma = -B\Delta\tau \tag{72}$$

The shear stress increment causing the reversed plasticity to occur can be found from Eq. (70) as

$$\Delta\tau_2 = -[2(g_2 - Bf_2)]/(1 + B^2) \tag{73}$$

Thus, the stresses when new plastic deformation begins will be

$$\sigma_3 = \sigma_2 + [2B(g_2 - Bf_2)]/(1 + B^2) \tag{74a}$$

$$\tau_3 = \tau_2 - [2(g_2 - Bf_2)]/(1 + B^2) \tag{74b}$$

Note that the yield center remains stationary during the unloading so that

$$\alpha_3 = \alpha_2 \tag{75a}$$

$$\beta_3 = \beta_2 \tag{75b}$$

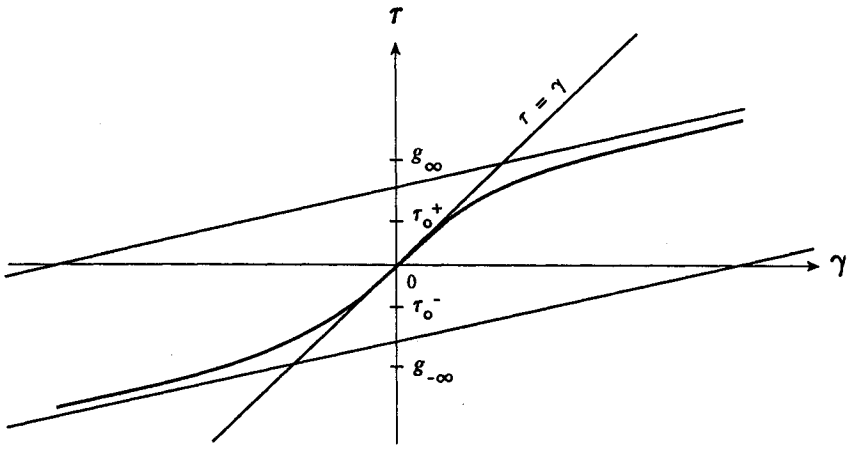

Fig. 6 Shear stress-strain relationship, linear stress path ($\sigma = A$).

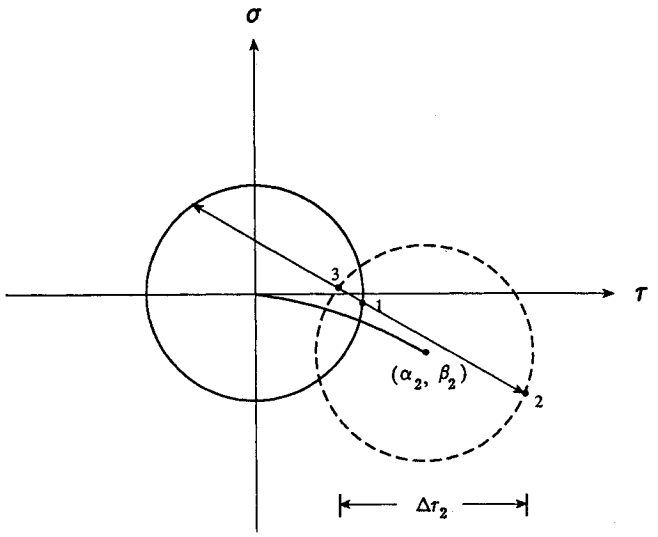

Fig. 7 Linear stress path ($\sigma = A - B\tau$, $B>0$), variable loading.

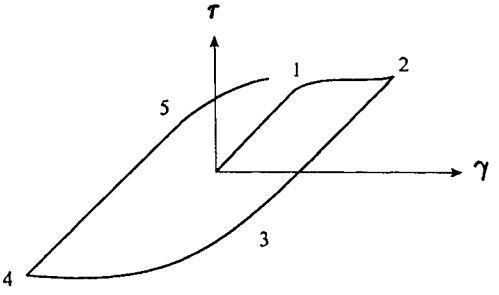

Fig. 8 Shear stress-strain loop for the first cycle, linear stress path ($\sigma = A - B\tau$, $B>0$).

As a result, at point 3

$$f_3 = \sigma_3 - \alpha_3 = \sigma_2 + \Delta\sigma_2 - \alpha_2 = f_2 + \Delta\sigma_2$$
$$= [(1 - B^2)f_2 + 2Bg_2]/(1 + B^2) \tag{76a}$$
$$g_3 = \tau_3 - \beta_3 = \tau_2 + \Delta\tau_2 - \alpha_2 = g_2 + \Delta\tau_2$$
$$= [2Bf_2 - (1 - B^2)g_2]/(1 + B^2) \tag{76b}$$

or

$$f_3 = (BX_2^2 + 2X_2 - B)/[\sqrt{1 + B^2}(X_2^2 + 1)] \tag{77a}$$
$$g_3 = -(X_2^2 - 2BX_2 - 1)/[\sqrt{1 + B^2}(X_2^2 + 1)] \tag{77b}$$

if use is made of Eq. (41). Now, the new initial condition for the X function will be

$$X_3 = -(B - \sqrt{1 + B^2}f_3)/(1 - \sqrt{1 + B^2}g_3) = 1/X_2 \tag{78}$$

where X_2 can be found from Eq. (42) for the first loading:

$$X_2 = X_0^+ \exp[\sqrt{1 + B^2}(\tau_2 - \tau_0)] \tag{79}$$

The yield center and the stress-strain relation during the reversed plasticity are still expressed by Eqs. (40) and (46), but based on a new X function:

$$X = X_3 \exp[\sqrt{1 + B^2}(\tau - \tau_3)] \tag{80}$$

Suppose that when the unloading continues up to the loading point 4 (Fig. 8), the tube is loaded in the positive loading direction again. Similarly, after loading point 5, where

$$\sigma_5 = \sigma_4 + [2B(g_4 - Bf_4)]/(1 + B^2) \tag{81a}$$
$$\tau_5 = \tau_4 - [2(g_4 - Bf_4)]/(1 + B^2) \tag{81b}$$
$$\alpha_5 = \alpha_4 \tag{82a}$$
$$\beta_5 = \beta_4 \tag{82b}$$

a new reversed plasticity process will take place. This time, it is a transition from negative deformation to positive deformation, and the new positive plastic deformation will be determined by a new X function

$$X = X_5 \exp[\sqrt{1 + B^2}(\tau - \tau_5)] \tag{83}$$

with initial condition

$$X_5 = 1/X_4 = X_0^+ \exp[\sqrt{1 + B^2}(-\tau_4 + \tau_3 + \tau_2 - \tau_0)] \tag{84}$$

If this kind of loading and unloading continues, we can find that for the nth positive plastic deformation (Fig. 9),

$$X = X_{4n-3} \exp[\sqrt{1 + B^2}(\tau - \tau_{4n-3})] \tag{85}$$

where

$$X_{4n-3} = X_0^+ \exp\left[-\sqrt{1 + B^2}\sum_{k=1}^{2(n-1)}(-1)^k(\tau_{2k} - \tau_{2k-1})\right] \tag{86}$$

For the nth negative plastic deformation

$$X = X_{4n-1} \exp[\sqrt{1 + B^2}(\tau - \tau_{4n-1})] \tag{87}$$

where

$$X_{4n-1} = (1/X_0^+)\exp\left[\sqrt{1 + B^2}\sum_{k=1}^{2n-1}(-1)^k(\tau_{2k} - \tau_{2k-1})\right] \tag{88}$$

The yield center and the stress-strain relationships are always determined by Eqs. (40) and (46), with the appropriate X function.

Note that $-(-1)^k(\tau_{2k} - \tau_{2k-1})$ is positive. Therefore, X_{4n-3} increases, while X_{4n-1} decreases with the loading-unloading cycles. For a very large n, X_{4n-3} and consequently the X function for the positive loading direction approaches infinity, while X_{4n-1} and consequently the X function for the negative loading direction approaches zero. By Eq. (41), the g function approaches g_∞ and $g_{-\infty}$, and the shear stress-strain curve approaches the asymptotes, Eqs. (58) and (66), respectively. The deviation thus shows that no matter how the forces vary, or how far the loading or unloading process extends, if every time we load or unload the tube until reversed plasticity takes place, and then change the loading direction, the stress-strain curve will finally be straightened after a large number of cycles. At that time, the shear stress-strain point (τ, γ) will move along parallelograms formed by two asymptotes, Eqs. (58) and (66), and two unloading straight lines determined by the loading and unloading stresses. The yield center will move along the stress path, following the loading point.

Tubes subjected to sustained internal pressure and cyclic axial force are often used in the experimental investigation of plastic deformation. Suppose that the axial force varies from $-P_a$ to P_a. Then, the shear stress will vary from τ^+ to $-\tau^-$, where, for the open-end tube

$$\tau^+ = (P_a + 2\pi a^2 p)/4\pi ah\tau_y \tag{89a}$$
$$\tau^- = (P_a - 2\pi a^2 p)/4\pi ah\tau_y \tag{89b}$$

and for the closed-end tube

$$\tau^+ = (P_a + \pi a^2 p)/4\pi ah\tau_y \tag{90a}$$
$$\tau^- = (P_a - \pi a^2 p)/4\pi ah\tau_y \tag{90b}$$

In such a case, we can find for the positive loading direction

$$X = X_{4n-3} \exp[\sqrt{1 + B^2}(\tau + \tau^- - \Delta\tau_{4n-4})] \tag{91}$$

with

$$X_{4n-3} = X_0^+ \exp\left\{\sqrt{1 + B^2}\left[2(n-1)\tau^+ + (2n-3)\tau^- - \tau_0 - \sum_{k=1}^{2n-3}(-1)^k\Delta\tau_{2k}\right]\right\} \tag{92}$$

For the negative loading direction

$$X = X_{4n-1} \exp[\sqrt{1 + B^2}(\tau - \tau^+ - \Delta\tau_{4n-2})] \tag{93}$$

with

$$X_{4n-1} = (1/X_0^+)\exp\left\{-\sqrt{1 + B^2}\left[(2n-1)\tau^+ + 2(n-1)\tau^- - \tau_0 - \sum_{k=1}^{2(n-1)}(-1)^k\Delta\tau_{2k}\right]\right\} \tag{94}$$

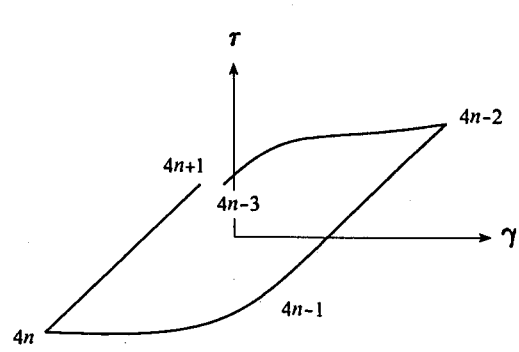

Fig. 9 Shear stress-strain loop for the nth cycle, linear stress path ($\sigma = A - B\tau$, $B > 0$).

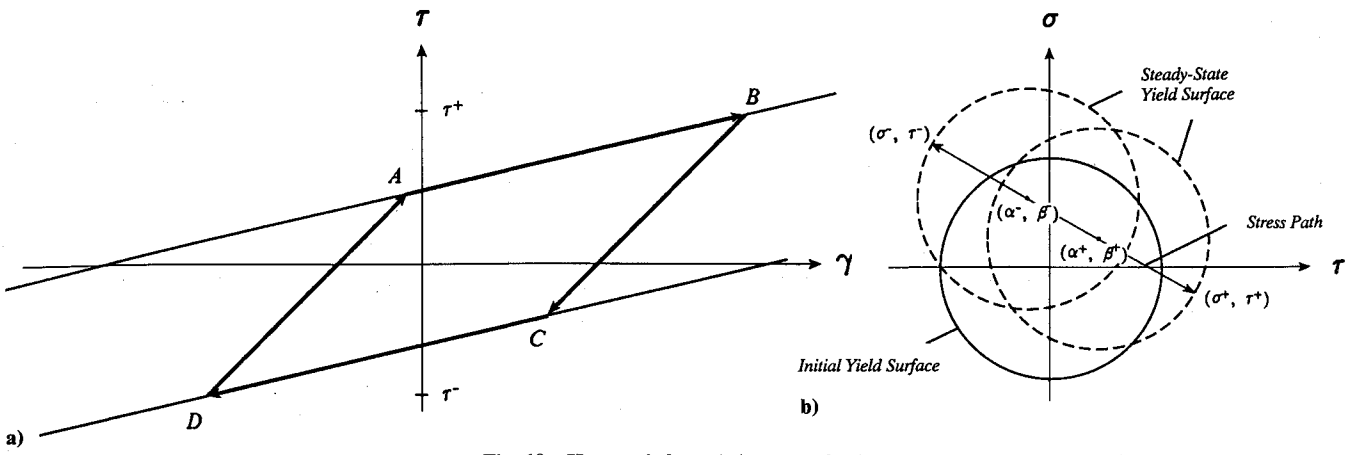

Fig. 10 Hysteresis loop ($\tau^+ + \tau^- > 2g_\infty$).

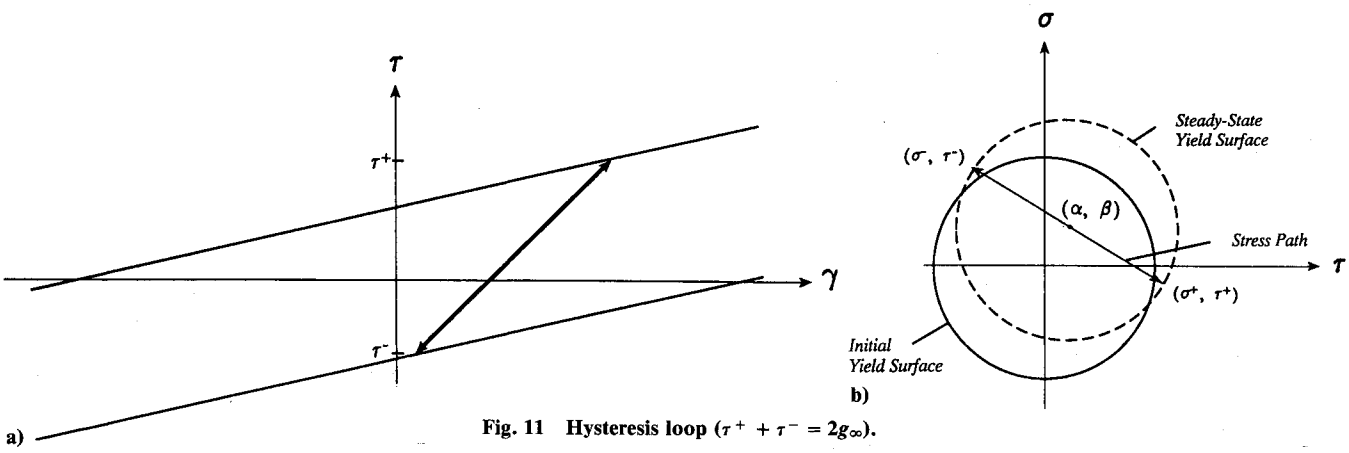

Fig. 11 Hysteresis loop ($\tau^+ + \tau^- = 2g_\infty$).

In Eqs. (91–94),

$$\Delta\tau_{2k} = -[2(X_{2k}^2 - 1)]/[\sqrt{1+B^2}(X_{2k}^2 + 1)] \tag{95}$$

Again, the X function will keep increasing for positive loading direction and keep decreasing for negative loading direction. Since the axial stress varies between two fixed limits, a stable hysteresis loop can be reached.

If the shear stress range $\tau^+ + \tau^- > 2g_\infty$, the reversed plasticity will always take place during the cycles, until the g function reaches $g_{\pm\infty}$. The hysteresis loop will be a parallelogram (Fig. 10a). The stress and strain at its four corners are

$$\tau_A = -\tau^- + 2/(\sqrt{1+B^2}) \tag{96a}$$

$$\tau_B = \tau^+ \tag{96b}$$

$$\tau_C = \tau^+ - 2/(\sqrt{1+B^2}) \tag{96c}$$

$$\tau_D = -\tau^- \tag{96d}$$

$$\gamma_A = -[1 + (2G/m)]\tau^- + [2/(\sqrt{1+B^2})][1 + (G/m)] \tag{97a}$$

$$\gamma_B = [1 + (2G/m)]\tau^+ - [2G/(m\sqrt{1+B^2})] \tag{97b}$$

$$\gamma_C = [1 + (2G/m)]\tau^+ - [2/(\sqrt{1+B^2})][1 + (G/m)] \tag{97c}$$

$$\gamma_D = -[1 + (2G/m)]\tau^- + [2G/(m\sqrt{1+B^2})] \tag{97d}$$

and by Eq. (40), the yield center (α, β) cycles along the stress path (Fig. 10b) from point

$$\alpha^+ = A - B\tau^+ + B/(\sqrt{1+B^2}) \tag{98a}$$

$$\beta^+ = \tau^+ - 1/(\sqrt{1+B^2}) \tag{98b}$$

to point

$$\alpha^- = A + B\tau^- - B/(\sqrt{1+B^2}) \tag{99a}$$

$$\beta^- = -\tau^- + 1/(\sqrt{1+B^2}) \tag{99b}$$

From Eqs. (97)

$$\gamma_B - \gamma_A = \gamma_C - \gamma_D = [1 + (2G/m)][\tau^+ + \tau^- - 2/(\sqrt{1+B^2})] \tag{100}$$

The shape of the hysteresis loop thus depends on the shear stress range.

In the case of shear stress range $\tau^+ + \tau^- = 2g_\infty$,

$$\gamma_B = \gamma_A \tag{101a}$$

$$\gamma_C = \gamma_D \tag{101b}$$

and the hysteresis loop degenerates to a straight line (Fig. 11a). The response of the tube becomes elastic. The yield surface no longer moves (Fig. 11b), with the yield center stationed at the point

$$\alpha = A - [B(\tau^+ - \tau^-)]/2 \tag{102a}$$

$$\beta = (\tau^+ - \tau^-)/2 \tag{102b}$$

If $\tau^+ + \tau^- < 2g_\infty$, reversed plasticity can no longer take place when the absolute value of the stress increment $\Delta\tau_{2k}$, which increases with each cycle, reaches or exceeds $\tau^+ + \tau^-$, that is, according to Eq. (95), when

$$[2(X_{2k}^2 - 1)/\sqrt{1+B^2}(X_{2k}^2 + 1)] \geq \tau^+ + \tau^- \tag{103}$$

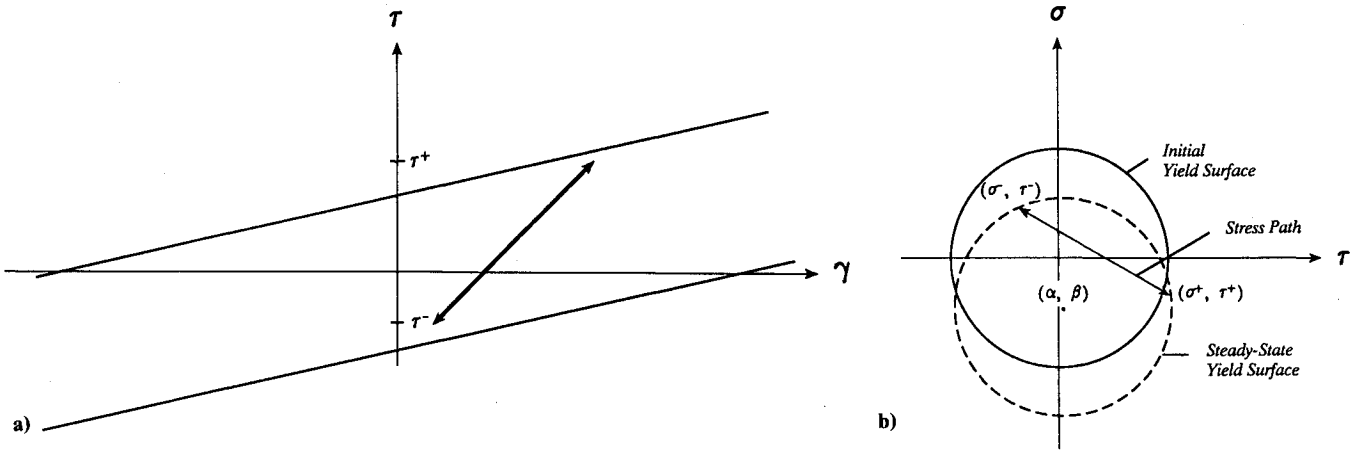

Fig. 12 Hysteresis loop ($\tau^+ + \tau^- < 2g_\infty$).

In such a case, the two functions f and g cannot fully develop to values $f_{\pm\infty}$ and $g_{\pm\infty}$.

If $\tau^+ + \tau^- \leq \Delta\tau_2$, the tube will elastically shake down immediately during the first unloading. The unloading point stays somewhere inside the yield surface, and the yield center stations at the point

$$\alpha = A - B\tau^+ - f_2 \tag{104a}$$

$$\beta = \tau^+ - g_2 \tag{104b}$$

If $\tau^+ + \tau^- > \Delta\tau_2$, the tube will incur repeated reversed plasticity before it can elastically shake down. When the steady state is reached, we can find by Eq. (103)

$$\alpha = A - \frac{1}{2}\left[B(\tau^+ - \tau^-) + \sqrt{\frac{4 - (1+B^2)(\tau^+ + \tau^-)^2}{1+B^2}}\right] \tag{105a}$$

$$\beta = \frac{1}{2}\left[(\tau^+ - \tau^-) - B\sqrt{\frac{4 - (1+B^2)(\tau^+ + \tau^-)^2}{1+B^2}}\right] \tag{105b}$$

The stress-strain loop degenerates to a straight line (Fig. 12a), and the loading point hit the yield surface twice during a cycle (Fig. 12b).

After the yield center is found from Eqs. (98), (99), (102), (104), or (105) for various cases, the steady-state residual strains (ϵ^p, γ^p) can be determined from Eq. (44), and then the strains (ϵ_ϕ, ϵ_z) can be determined from Eq. (31).

Note that in the negative loading direction, the g function is always monotonically decreased, concave upward. In the positive loading direction, the g function is initially monotonically increased, concave downward before it changes to become monotonically decreased and then concave upward (Fig. 3b). Therefore, during negative loading the plastic shear strain always increases. During the positive loading, depending on the location and direction of the stress path, the plastic shear strain can decrease first before it finally increases with each cycle. In other words, the left side of the shear stress-strain loop always moves to the right, whereas the right side of the loop, in some cases, will move to the left at the beginning, and then moves to the right together with the left side until the steady state is reached. From Eqs. (102), it is seen that the plastic shear strain will totally disappear when $\tau^+ = \tau^- = g_\infty$. Otherwise, there will always be residual strains.

The variation of the f function is shown in Fig. 3a. It decreases monotonically for large shear stress. As a result, the plastic strain ϵ^p will grow insistently during the cycles.

VI. Proportional Loading

Consider now the stress path

$$\sigma = -B\tau \tag{106}$$

that is, consider the case where the stress components vary in proportion to each other.

In such a case, plasticity will first start when the loading point reaches (σ_0, τ_0), where

$$\sigma_0 = \mp (B/\sqrt{1+B^2}) \tag{107a}$$

$$\tau_0 = \pm (1/\sqrt{1+B^2}) \tag{107b}$$

and the solution to the differential equation, Eq. (39), can be found as

$$\alpha = -B\beta \tag{108a}$$

$$\beta = \tau - \tau_0 \tag{108b}$$

$$\epsilon = \{1 + E/[3m(1-\nu)]\}\sigma + EB/[3m(1-\nu)]\tau_0 \tag{109a}$$

$$\gamma = [1 + (2G/m)]\tau - (2G/m)\tau_0 \tag{109b}$$

It is seen that in the case of proportional loading, the yield center moves along the stress path and the stress-strain relationships are simply bilinear and are identical to the relationships represented by the asymptotes, Eqs. (58) and (66). Note that the nonproportional shear stress-strain curve for the positive loading direction exceeds the asymptote, Eq. (58), for a stress path with a positive B value (Fig. 4). The nonproportional shear stress-strain curve for the negative loading direction falls below the asymptote, Eq. (66), for a stress path with a negative B value. These facts show that the material exhibits extra hardening during the nonproportional loading rather than during the proportional loading. However, such extra hardening associated with the linear kinematic rule is a transient effect, which fades with loading cycles.

VII. Conclusions

The elastic-plastic analysis of machines and structures subjected to variable loads and temperatures depends extensively on the constitutive laws employed. Recent experimental investigations indicate that the materials exhibit various complicated behaviors in nonproportional loading other than those in proportional loading. Such situations lead to demands for a careful review of the available constitutive equations and development of new models.

Because of the complexity of the triaxial stress test, most experiments were performed on the state of plane stress using thin-walled tubes subjected to combined axial force and twisting moment ($P + M$ test), or combined axial force and internal pressure ($P + p$ test). A theoretical analysis of the $P + M$ test based on the ideal plasticity theory can be found in Ref. 6. Megahed[7] studied the influence of various hardening rules on the steady-state cyclic plasticity of the pressurized tube sub-

jected to cycles of push-pull. This paper presents a thorough investigation of both the transient and steady-state behaviors of the tube along linear internal pressure-axial force paths.

This paper proves the experimental findings that the material behaves quite differently under different loading situations. The response of the tube under nonproportional loading is shown to be strongly path-dependent, and the material exhibits higher hardening in some directions as compared with the proportional loading situation. The stress-strain curve is always monotonically increased as can be expected. However, its shape varies with the loading path. In some directions, it is initially concave downward and then changes to concave upward, exhibiting a yield plateau as commonly found in the test. The movement of the yield center and variation of the stress-strain loop are discussed in detail in the paper. The shear stress-strain loop is shown to always move to the right after a large number of cycles, indicating the strain growth. Depending on the loading path, however, it is also possible that the right side of the shear stress-strain loop moves to the left during the initial cycles. As a result, in some cases the stress-strain loop can degenerate to a straight line. The residual strain can even totally disappear. The paper then shows that the differences between nonproportional and proportional loading behaviors will finally disappear if the tube is loaded in some specific direction or if it is subjected to cyclic loading when the steady state, either one of the elastic shakedown or one of the cyclic reversed plasticity, is reached.

This research obtains analytical closed-form solutions to the thin-walled tube subjected to combined internal pressure and axial load. Based on that, this paper provides detailed information as to how the classic linear kinematic hardening rule describes the material behavior under nonproportional loadings. It appears that this simple model is able to describe some of the basic characteristics of the material behavior observed in nonproportional tests. However, it is only by comparing with test data obtained under the same geometric and loading conditions as discussed in this paper that a conclusion can be made as to how well this simple model predicts the material behavior.

References

[1]Lamba, H. S., and Sidebottom, O. M., "Cyclic Plasticity for Nonproportional Paths: Pt. 1—Cyclic Hardening, Erasure of Memory, and Subsequent Strain Hardening Experiments," *Journal of Engineering Materials Technology,* Vol. 100, 1978, p. 96.

[2]Lamba, H. S., and Sidebottom, O. M., "Cyclic Plasticity for Nonproportional Paths: Pt. 2—Comparison with Predictions of Three Incremental Plasticity Models," *Journal of Engineering Materials Technology,* Vol. 100, 1978, p. 104.

[3]McDowell, D. L., "On the Path Dependence of Transient Hardening and Softening to Stable State Under Complex Biaxial Loading," *Proceedings of the International Conference on Constitutive Laws for Engineering Materials,* edited by Desai and Gallagher, Tucson, AZ, 1983, pp. 125–132.

[4]Jie, N., and Xu, C., "On the Properties of Plastic Flow of Material under Nonproportional Cyclic Loading," *International Journal of Solids and Structures,* Vol. 28, No. 4, 1991, pp. 403–412.

[5]Xia, Z., and Ellyin, F., "Nonproportional Multiaxial Cyclic Loading: Experiments and Constitutive Modeling," *Journal of Applied Mechanics,* Vol. 58, No. 2, 1991, pp. 317–325.

[6]Kachanov, L. M., *Fundamentals of the Theory of Plasticity,* Mir Publishers, Moscow, 1974, pp. 77–80.

[7]Megahed, M. M., "Influence of Hardening Rule on Prediction of Cyclic Plasticity in Pressured Thin Tubes Subjected to Cyclic Push-Pull," *International Journal of Mechanical Science,* Vol. 32, No. 8, 1990, pp. 635–652.